01 Sep 2018

Deformation of a Ferrofluid Droplet in Simple Shear Flows under Uniform Magnetic Fields

Md Rifat Hassan

Jie Zhang

Cheng Wang
Missouri University of Science and Technology, wancheng@mst.edu

Recommended Citation

M. R. Hassan et al., "Deformation of a Ferrofluid Droplet in Simple Shear Flows under Uniform Magnetic Fields," *Physics of Fluids*, vol. 30, no. 9, American Institute of Physics (AIP), Sep 2018.
The definitive version is available at https://doi.org/10.1063/1.5047223

Deformation of a ferrofluid droplet in simple shear flows under uniform magnetic fields

Md Rifat Hassan, Jie Zhang, and Cheng Wang[a)]
Department of Mechanical and Aerospace Engineering, Missouri University of Science and Technology, 400 West 13th St., Rolla, Missouri 65409, USA

(Received 5 July 2018; accepted 23 August 2018; published online 11 September 2018)

We numerically investigate the deformation and orientation of a ferrofluid droplet in a simple shear flow under a uniform magnetic field. The numerical simulation is based on the finite element method and couples the magnetic and flow fields. A level set method is used to model the dynamic motion of the droplet interface. Systematic numerical simulations are used to assess the effects of the direction and the strength of the magnetic field. Focusing on low Reynolds number flows ($\mathrm{Re} \lesssim 0.02$), the numerical results indicate that at a small capillary number ($\mathrm{Ca} \approx 0.02$), the magnetic field dominates over the shear flow above a certain magnetic bond number ($\mathrm{Bo}_m \approx 3$). The orientation of the droplet is aligned with the direction of the magnetic field, while the deformation of the droplet varies slightly when the direction of the magnetic field is varied. On the other hand, for large capillary numbers ($\mathrm{Ca} \approx 0.23$), the deformation and orientation of the droplet is influenced by both the shear flow and the magnetic field, except for a small magnetic bond number ($\mathrm{Bo}_m \lesssim 0.2$). In both the small and large capillary number cases, the droplet deformation is found to be maximum at $\alpha = 45°$ (the direction of magnetic field) and minimum at $\alpha = 135°$. In addition, the effect of the magnetic field on the flow field inside and outside the droplet at different conditions is examined. We demonstrate active control of lateral migration of ferrofluid droplets in wall-bounded simple shear flows. The direction of the lateral migration depends on the orientation of the deformed droplets due to uniform magnetic fields at different directions. *Published by AIP Publishing.* https://doi.org/10.1063/1.5047223

I. INTRODUCTION

Emulsions are liquid droplets dispersed in another immiscible liquid phase. When subjected to shear flows, the droplets deform and may break up. Understanding the dynamics of droplets in shear flows is of great importance to a variety of technological and industrial applications that utilize emulsions, including cosmetics, food production, and polymer processing.[1,2] For example, in blending of molten polymers, the distribution of the droplet size and shape is critical to the rheology and physical properties of the polymer system.[3–5]

A single droplet in a simple shear flow serves as an excellent model problem to understand droplet dynamics and can provide fundamental insights into more complex emulsion systems.[6,7] Following the pioneering work of Taylor,[8,9] numerous experimental,[10–12] theoretical,[13] and numerical studies[14–17] have been carried out to investigate the deformation and breakup of a Newtonian droplet suspended in a shear flow of another viscous Newtonian fluid. Three-dimensional single-droplet deformation and breakup under a simple shear flow using numerical simulation has been investigated by Xi.[14] Debruijn[18] developed a Couette device to study the breakup of non-Newtonian droplets in a quasi-steady simple shear flow. Li[15] performed a numerical simulation using the volume of fluid (VOF) method to observe the breakup of a single droplet into daughter droplets via an end-pinching mechanism. Feigl[17] conducted both simulations and experiments to study the deformation and orientation of the droplet in a simple shear flow. These investigations find that the droplet deformation depends on several dimensionless parameters, including the capillary number, Reynolds number, viscosity ratio between the dispersed and continuous phases, and the confinement ratio. For a comprehensive review of this topic, readers are referred to a number of excellent review articles.[6,7]

In addition to using viscous shear, external force fields such as electric or magnetic fields provide an additional means of controlling the deformation of droplets.[19] When the droplets and suspending fluid have different electrical properties, an electric field will result in additional Maxwell stresses on the fluid interface to affect the droplet deformation.[20,21] Vlahovska[21] developed an analysis to describe the effect of a uniform electric field on the deformation and orientation of dielectric droplets in a simple shear flow. Mählmann *et al.*[20] investigated the electric field effects on two dimensional drops in a simple shear flow at arbitrary Reynolds numbers. Mandal[22] analytically studied the effect of a uniform electric field on the motion of droplet in an unbounded Poiseuille flow and also in a simple shear flow.[23]

Magnetic fields have been demonstrated to control the dynamics of single ferrofluid droplets[24,25] or emulsion systems.[26–28] To use magnetic manipulation, either the droplet or suspending fluid needs to be a ferrofluid[29]—a dispersion of magnetic nanoparticles (typical diameter around 10 nm and typical volume fraction 5%). Multiphase ferrofluid droplets have promising biomedical applications due to their ability

a)Electronic mail: wancheng@mst.edu

to be delivered at a specific site with the help of proper manipulation of a magnetic field. A notable biomedical application is the treatment of retinal detachment[30] by guiding a ferrofluid droplet inside the retinae. The magnetic field has also been extensively used in microfluidics to control the various manipulation of microdroplets. Varma *et al.* studied the magnetic field experimentally inducing the merging of droplets on a lab-on-a-chip application.[31] Liu *et al.* and Wu *et al.* studied the ferrofluid droplet formation under a uniform magnetic field.[32,33] Tan *et al.* reported the manipulation of a ferrofluid droplet at a microfluidic T-junction by using magnetic fields induced by permanent magnets.[34] Recently, Zhang *et al.* studied the flow regimes of ferrofluid droplets under a nonuniform magnetic field.[35]

To understand the role of the magnetic field, researchers have numerically and experimentally investigated the motion and deformation of a ferrofluid droplet suspended in a viscous medium under different flow conditions. Ghaffari[36] performed numerical simulations to study the equilibrium shape and coalescence behavior of suspended ferrofluid droplets under a uniform magnetic field. Bacri[24] studied the deformation of large magnetic agglomerates of a ferrofluid that are sandwiched in a Hele-Shaw cell in a weak magnetic field. Afkhami *et al.*[25,37] numerically investigated the deformation of a neutrally buoyant hydrophobic ferrofluid droplet in a viscous medium under a uniform magnetic field. Afkhami *et al.* also investigated the motion of a ferrofluid droplet in an axisymmetric geometry under a uniform magnetic field. Shi[38] numerically investigated the dynamics of a ferrofluid droplet falling in a non-magnetic fluid under a uniform magnetic field. Korlie[39] studied the rising of a bubble and sinking of a droplet in a ferrofluid by considering the gravity effect, while Zhu *et al.*[40] studied the nonlinear deformation of large ferrofluid droplets under the influence of a uniform magnetic field and gravity.

However, until now, few have studied the deformation of ferrofluid droplets in a simple shear flow under the influence of a uniform magnetic field. Recently, Jesus *et al.*[41] performed a three-dimensional numerical analysis on the droplet dynamics and field induced deformation of a ferrofluid droplet in another Newtonian fluid. They investigated the influence of the magnetic field on the time evolution of the droplet deformation for low shear rate and found that the presence of the magnetic field causes the deformation a longer time to reach a steady state. Their results suggest that at a fixed low shear rate, the magnetic field takes control of the deformation and orientation of the droplet at a higher magnetic bond number, Bo_m. Further, they found that for $\mathrm{Bo}_m \approx \mathcal{O}(1)$ and small Ca, the droplet deformation in the vorticity direction can be of the same order as that occurring in the shear plane. One advantage of using magnetic fields, when compared to electric fields, is that magnetic fields can be applied at arbitrary directions with ease. However, the existing investigations on magnetic control have primarily focused on either the field direction perpendicular and/or parallel to the flow direction[32,41] or a droplet in a quiescent flow.[24,25,36,39] A thorough understanding of the deformation dynamics of a ferrofluid droplet under both shear flows and magnetic fields is missing.

By using two-dimensional (2D) direct numerical simulations, this paper investigates the dynamics and deformation of a ferrofluid droplet in a simple shear flow under a uniform magnetic field that is focused in an arbitrary direction. For computational efficiency, we have chosen to use 2D simulations in order to study a wide range of parameters (i.e., capillary number, magnetic bond number, and field direction). Prior studies have shown that 2D numerical simulations are able to qualitatively and correctly capture the characteristics of droplet deformations in simple shear flows and droplet deformation under uniform magnetic fields.[4,38,42,43] Our numerical simulation, built with a commercial FEM solver, models the dynamic deformation of droplet interface by using the level set method and couples the magnetic and flow fields.

The remainder of this paper is organized as follows: in Sec. II, the mathematical model and numerical method are described. In Sec. III, we first present the numerical results obtained from the droplet deformation in a simple shear flow only and the droplet deformation under a uniform magnetic field, and we validate our numerical model against existing theories. We then examine the effect of the magnetic field on the droplet deformation and orientation by varying the field direction, magnetic bond number, and capillary number. Furthermore, by combining wall-bound simple shear flows and uniform magnetic fields, we demonstrate a versatile control of lateral migration motions of the ferrofluid droplets by adjusting the direction of the magnetic field. Finally, major findings are summarized in Sec. IV.

II. NUMERICAL SIMULATION METHOD

A. Level set method

In our model, we have used the conservative level set method to track the dynamic evolution of the interface between the droplet and suspending medium.[43,44] The level set function ϕ is an auxiliary scalar function used to represent the phases of the two fluids: In the droplet phase as $\phi = 1$ and in the continuous phase as $\phi = 0$. The value of ϕ smoothly transits from 0 to 1 over the interface, and here $\phi = 0.5$ is used to define the position of the interface. The level set function ϕ is advected by the velocity field by[45,46]

$$\frac{d\phi}{dt} + \mathbf{u}\cdot\nabla\phi = \gamma\nabla\cdot\left(\epsilon\nabla\phi - \phi(1-\phi)\frac{\nabla\phi}{|\nabla\phi|}\right), \tag{1}$$

where $\mathbf{u}$, γ, and ϵ denote the velocity field, the amount of reinitialization, and the thickness of the interface, respectively. The terms on the left-hand side of the equation represent the motion of the interface, while the terms on the right-hand side are required for numerical stability. The parameter ϵ defines the thickness of the interface and is set to equal the largest size of the mesh in the domain. The amount of stabilization is defined by the parameter γ, which needs to be carefully controlled for maintaining the thickness of the interface, and the appropriate value of γ is the maximum magnitude of the velocity field. The level set function ϕ can be used to find the unit normal to the interface $\mathbf{n}$,

$$\mathbf{n} = \frac{\nabla\phi}{|\nabla\phi|}. \tag{2}$$

With the level set method, the two immiscible fluids are treated as a single phase flow with material properties that vary according to the level set value. Here, a linear average is used, and the density (ρ), dynamic viscosity (η), magnetic permeability (μ), and magnetic susceptibility (χ) are related to ϕ via the following equations:

$$\rho = \rho_c + (\rho_d - \rho_c)\phi, \qquad \eta = \eta_c + (\eta_d - \eta_c)\phi, \tag{3}$$

$$\mu = \mu_c + (\mu_d - \mu_c)\phi, \qquad \chi = \chi_c + (\chi_d - \chi_c)\phi, \tag{4}$$

where the subscripts c and d represent the continuous phase and droplet phase, respectively.

B. Governing equations

The motion of an incompressible, immiscible ferrofluid droplet in another incompressible, immiscible medium under the effect of a uniform magnetic field is governed by the continuity and momentum equations,

$$\nabla \cdot \mathbf{u} = 0, \tag{5}$$

and

$$\rho\left(\frac{\partial \mathbf{u}}{\partial t} + \mathbf{u} \cdot \nabla \mathbf{u}\right) = -\nabla p + \nabla \cdot \boldsymbol{\tau} + \mathbf{F}_\sigma + \mathbf{F}_m, \tag{6}$$

where p denotes the pressure, $\boldsymbol{\tau} = [\eta(\nabla \mathbf{u} + (\nabla \mathbf{u})^T)]$ denotes the viscous stress, $\mathbf{F}_\sigma$ represents the force due to surface tension, and $\mathbf{F}_m$ represents the force due to the magnetic field.

The surface tension force $\mathbf{F}_\sigma$ is defined as

$$\mathbf{F}_\sigma = \nabla \cdot [\sigma\{\mathbf{I} + (-\mathbf{n}\mathbf{n}^T)\}\delta], \tag{7}$$

where σ is the coefficient of surface tension, $\mathbf{I}$ is the second-order identity tensor, δ is the Dirac delta function, and $\mathbf{n}$ is the unit normal to the interface that can be calculated using Eq. (2). The Dirac delta function δ is approximated using the level set function as

$$\delta = 6|\phi(1-\phi)||\nabla\phi|. \tag{8}$$

The magnetic force can be calculated as[29]

$$\mathbf{F}_m = \nabla \cdot \boldsymbol{\tau}_m = \nabla \cdot (\mu \mathbf{H}\mathbf{H}^T - \frac{\mu}{2}H^2\mathbf{I}), \tag{9}$$

where $\boldsymbol{\tau}_m$ is the magnetic stress tensor for the applied magnetic field and $H^2 = \mathbf{H} \cdot \mathbf{H} = |\mathbf{H}|^2$. To calculate the magnetic stress tensor, the magneto-statics equations, including magnetic induction $\mathbf{B}$, magnetization $\mathbf{M}$, and magnetic field $\mathbf{H}$, are solved. Assuming linear and homogeneous material properties, the magneto-static Maxwell equation relates $\mathbf{B}$, $\mathbf{H}$, and $\mathbf{M}$ via the following relationships:[47]

$$\nabla \cdot \mathbf{B} = 0, \qquad \nabla \times \mathbf{H} = 0, \qquad \mathbf{M} = \chi\mathbf{H}, \quad \text{and} \quad \mathbf{B} = \mu_0(\mathbf{H} + \mathbf{M}) = \mu_0(1+\chi)\mathbf{H}, \tag{10}$$

where $\mu_0 = 4\pi \times 10^{-7}$ N/A^2 is the permeability of vacuum and μ and χ depend on the phase function ϕ according to Eq. (4). A scalar potential ψ can be defined, and its gradient represents curl-free $\mathbf{H}$ (i.e., $\mathbf{H} = -\nabla\psi$). We can now write

$$\nabla \cdot (\mu \nabla \psi) = 0. \tag{11}$$

C. Governing equations in non-dimensional form

We rewrite the governing equations to understand the main effects (in terms of dimensionless groups) that control the droplet dynamics. We scale the length by the radius of the initially undeformed droplet (R_0) and time by the inverse of shear rate $\frac{1}{\dot{\gamma}}$, respectively. The other dimensionless variables are defined as follows:

$$p^* = \frac{p}{\eta\dot{\gamma}}, \quad \rho^* = \frac{\rho}{\rho_c}, \quad \eta^* = \frac{\eta}{\eta_c}, \quad \mu^* = \frac{\mu}{\mu_0}, \quad \mathbf{H}^* = \frac{\mathbf{H}}{H_0},$$

where H_0 is the magnitude of the externally applied magnetic field $\mathbf{H}_0$. Therefore, the governing equations (5) and (6) can be written as

$$\nabla^* \cdot \mathbf{u}^* = 0, \tag{12}$$

$$\mathrm{Re}\left(\rho^* \frac{D\mathbf{u}^*}{Dt^*}\right) = -\nabla^* p^* + \nabla^* \cdot \tau^* + 2\frac{\mathrm{Bo}_m}{\mathrm{Ca}}\nabla^* \cdot \boldsymbol{\tau}_m^* + \frac{1}{\mathrm{Ca}}\mathbf{F}_\sigma^*. \tag{13}$$

In the above equation, the superscript $(*)$ represents the nondimensional variables and Re, Ca, and Bo_m represent the Reynolds number, capillary number, and magnetic bond number, respectively, which are defined as follows:

$$\mathrm{Re} = \frac{\rho_c {R_0}^2 \dot{\gamma}}{\eta_c}, \tag{14}$$

$$\mathrm{Ca} = \frac{\eta_c R_0 \dot{\gamma}}{\sigma}, \tag{15}$$

and

$$\mathrm{Bo}_m = \frac{R_0 \mu_0 {H_0}^2}{2\sigma}. \tag{16}$$

Other nondimensional groups, including the viscosity ratio λ and permeability ratio ζ, are defined as follows:

$$\lambda = \frac{\eta_d}{\eta_c} \quad \text{and} \quad \zeta = \frac{\mu_d}{\mu_0}. \tag{17}$$

Note that the ratio between Bo_m and Ca is known as the Mason number, Mn. By restricting to low Reynolds number flows ($\mathrm{Re} \lesssim 0.02$), we will mainly concentrate on the effects of Ca, Bo_m, and the direction of the magnetic field on the deformation and orientation of the droplet.

D. Numerical model

Figure 1 schematically depicts a ferrofluid droplet (with magnetic susceptibility $\chi_d = 1$) suspended in another nonmagnetic ($\chi_c = 0$) viscous fluid medium in a simple shear flow under the application of a uniform magnetic field, $\mathbf{H}_0$. The height and width of the computational domain are $H_{domain} = W_{domain} = 10R_0$, where $R_0 = 50$ μm is the radius of the initially undeformed droplet. The viscosity and density of both the phases are considered equal to each other (i.e., $\eta_c = \eta_d$) where the value of the viscosity was equal to 0.105 Pa s. The coefficient of surface tension is considered as $\sigma = 0.0135$ N/m.

Initially, the ferrofluid droplet was placed at the center of the computational domain. The top wall moves with a velocity $\mathbf{u}_t = \frac{1}{2}\dot{\gamma}H_{domain}\mathbf{e}_x$, and the bottom wall moves with a

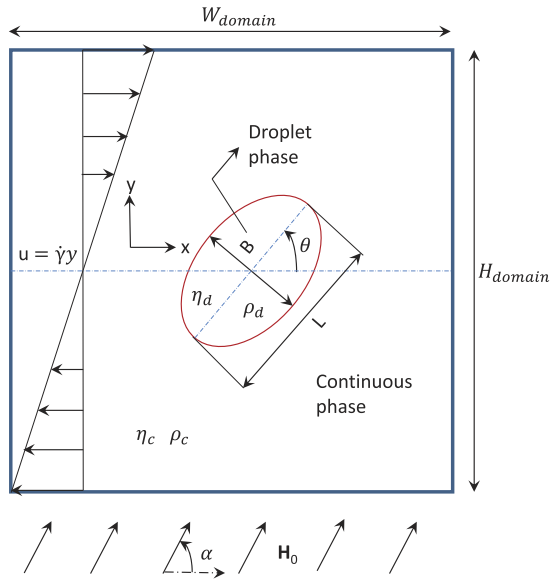

FIG. 1. Schematic illustration of a ferrofluid droplet suspended in another viscous fluid in a simple shear flow under a uniform magnetic field, $\mathbf{H}_0$.

velocity $\mathbf{u}_b = -\frac{1}{2}\dot{\gamma}H_{domain}\mathbf{e}_x$, thus resulting in a simple shear flow with the constant shear rate $\dot{\gamma}$. Periodic flow condition was applied to both the left and right walls in the x-direction. A uniform magnetic field, $\mathbf{H}_0$, was applied to the flow domain along an arbitrary direction, which is denoted by the angle α. The deformed droplet is characterized by the largest and smallest dimensions, L and B, along the major-axis and minor-axis, respectively. The orientation angle of the deformed droplet θ is defined as the angle measured in the counterclockwise direction from the positive x-direction to the major axis of the droplet.

E. Grid independence test

We carried out a grid independence test to determine optimal mesh sizes that give accurate results while using less computational time. For this validation, the simulation used different mesh sizes and compared the deformation of the ferrofluid droplet for each case. The magnetic field was applied at 45° to the flow domain ($\alpha = 45°$). Table I gives different mesh sizes for the grid independence test, and Fig. 2 illustrates the deformation parameter $D = \frac{L-B}{L+B}$ of the ferrofluid droplet against time for these respective mesh sizes. We used free triangular elements for creating the mesh in the domain. It can be seen that when there are greater than 26 536 elements in the flow field domain, the results for the ferrofluid droplet deformation tend to superimpose on each other. In the remainder of this paper, we have used 42 616 elements for the flow field domain to perform numerical simulations.

TABLE I. Different mesh sizes for grid independence test.

	Mesh 1	Mesh 2	Mesh 3	Mesh 4	Mesh 5	Mesh 6
Flow field domain	16 000	19 888	26 536	29 008	33 392	42 616

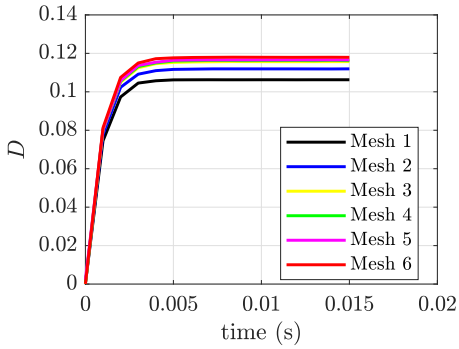

FIG. 2. Grid independence test: the time evolution of the deformation parameter, D, of a ferrofluid droplet with different mesh settings.

III. RESULTS AND DISCUSSIONS

A. Validation of numerical method

1. Droplet in a simple shear flow

We first validated our model by simulating the droplet deformation in a simple shear flow only and compared the numerical results with existing theories and experimental data in terms of the deformation parameter D and the orientation angle θ. According to Taylor,[8,9] the deformation parameter of a neutrally buoyant droplet suspended in another viscous fluid under a simple shear at the Stokes flow limit can be calculated as

$$D = \frac{L-B}{L+B} = \frac{19\eta_d + 16\eta_c}{16\eta_d + 16\eta_c}\mathrm{Ca}, \tag{18}$$

where the capillary number Ca is defined in Eq. (15). Equation (18) is based on the assumption of an unbounded simple shear flow and a vanishing Reynolds number. In numerical studies, however, the simple shear flow is achieved by moving two confining walls, thus giving rise to the so-called confinement effect, which is characterized by the confinement ratio $\frac{2R_0}{H}$. Kennedy[48] and Guido[49] reported that the confinement effect is negligible on the deformation of the droplet when $\frac{2R_0}{H} < 0.4$. In our model, $\frac{2R_0}{H} = 0.2$, and thus, the confinement effect can be neglected.

Figure 3(a) shows the equilibrium droplet shapes under different capillary numbers. The deformation of the droplet increases with increasing Ca. Figure 3(b) represents the comparison of the simulation results with Taylor's theory and the experimental results of Vananroye *et al.*[50] When Ca < 0.15, the simulation results and Taylor's theory agree very well with each other although the experimental results are slightly larger at all capillary numbers compared to the theoretical results. When the capillary number is large (Ca > 0.15), the difference between the numerical simulations and the theoretical prediction increases. This discrepancy could be attributed to the nature of two-dimensional simulation.[4] Nevertheless, the numerical results are considered satisfactory since the errors are within a few percent. For example, when the capillary number was equal to 0.2333, the error between the deformation of the ferrofluid droplet of the simulation results with respect to Taylor's theory was approximately 8%.

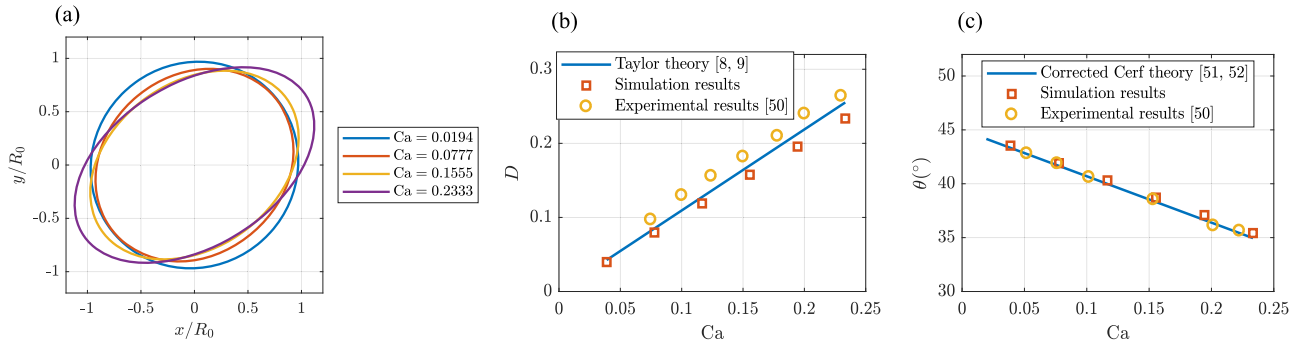

FIG. 3. Droplet deformation in a simple shear. (a) Outline of the droplet; (b) comparison of simulation results against Taylor's theory[8,9] and the experimental results of Vananroye *et al.*,[50] D vs Ca; and (c) comparison of simulation results against the corrected Cerf's theory[51,52] and experimental results of Vananroye *et al.*,[50] θ vs Ca for $\lambda = 0.3$.

We also evaluated the orientation angle of the droplet θ for the different cases and compared our results with the corrected Cerf[51,52] theory and the experiments performed by Vananroye *et al.*[50] According to the theory,[52] the orientation angle in a simple shear flow is

$$\theta = \frac{\pi}{4} - D\frac{3+2\lambda}{5}. \tag{19}$$

In our numerical results, the orientation angle θ was found to be 43.537° and 35.424° when the capillary number was equal to 0.0388 and 0.2333, respectively. Figure 3(c) shows the comparison of the orientation angle θ for different capillary numbers, Ca, between the simulation results, the corrected Cerf theory, and the experimental results, illustrating very good agreement with each other.

2. Droplet deformation under a uniform magnetic field in a quiescent flow

We further validated our model for the deformation of the ferrofluid droplet in a quiescent fluid under a uniform magnetic field. For this purpose, we used the theory provided by Afkhami *et al.*[25] According to them, the magnetic bond number Bo_m is related to the deformation of a ferrofluid droplet by the following relationship:

$$\mathrm{Bo}_m = \left(\frac{1}{\chi} + k\right)^2 \left(\frac{b}{a}\right)^{\frac{1}{3}} \left[2\frac{b}{a} - \left(\frac{b}{a}\right)^{-2} - 1\right], \tag{20}$$

where $\frac{b}{a}$ is the aspect ratio of the droplet by assuming an ellipsoidal droplet (i.e., $\frac{b}{a} = \frac{L}{B}$) and k is the demagnetizing factor,

$$k = \left(\frac{1-E^2}{2E^3}\right)\left(\ln\frac{1+E}{1-E} - 2E\right), \tag{21}$$

with E being the eccentricity of the ferrofluid droplet, which is given by

$$E = \sqrt{1 - \frac{a^2}{b^2}}. \tag{22}$$

We determined the deformation of the droplet for different magnetic bond numbers from the numerical simulations. For this case, we applied the magnetic field along the y axis (i.e., $\alpha = 90°$). Figure 4(a) indicates that with the increase in magnetic field strengths, the droplet is elongated more along the direction of magnetic field, and its steady-state shapes are approximately elliptical for Bo_m up to 10. Moreover, it can be seen from Fig. 4(b) that the simulation results agree well with the theory of Afkhami *et al.* for $\mathrm{Bo}_m \leq 7$. As the magnetic bond number Bo_m increases (i.e., $\mathrm{Bo}_m \approx 10$), the deformation of the droplet from our numerical simulation deviates more from the theoretical prediction. Even so, the difference between the numerical results and the theoretical prediction is within a few percent. For example, when the magnetic bond number Bo_m was equal to 9.83, the error for the ferrofluid droplet deformation parameter D between the simulation results and theory derived by Afkhami *et al.* was approximately 5%.

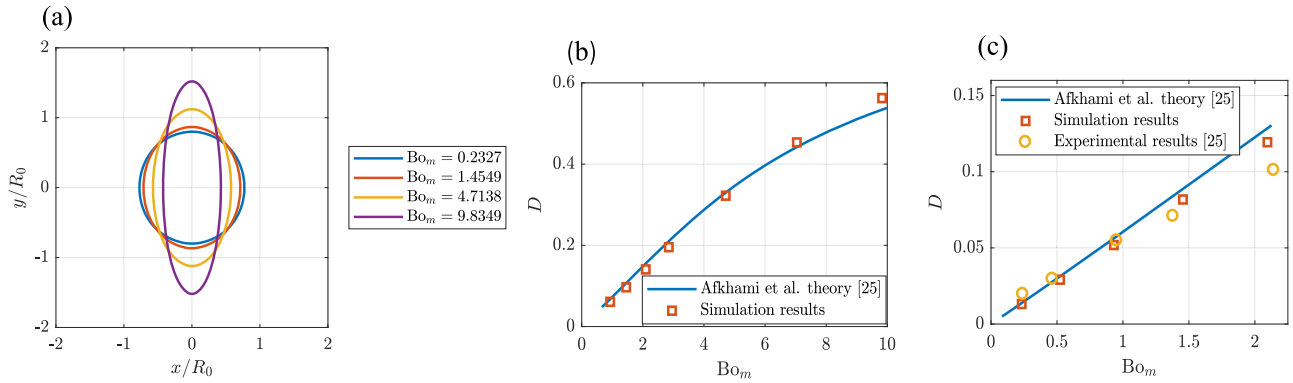

FIG. 4. Deformation of a ferrofluid droplet in a uniform magnetic field. (a) Equilibrium shape of the droplet; (b) comparison of the deformation parameter D vs Bo_m between the numerical simulation and the Afkhami *et al.* theory;[25] and (c) comparison of simulation results against the Afkhami *et al.* theory[25] and experimental results[25] for low magnetic field data with $\chi = 0.89$.

One of the reasons behind this discrepancy could be that the theory is based on an axisymmetric droplet. While we consider a two-dimensional droplet in the numerical simulation. We also compared our numerical results against the theory and experiments done by Afkhami *et al.*[25] for low magnetic field data. Figure 4(c) shows that our simulation results are consistent with both the theoretical results and the experimental results, except at a magnetic bond number $\mathrm{Bo}_m > 2$. The difference in the theoretical and simulation results with the experimental results at a magnetic bond number $\mathrm{Bo}_m > 2$ could be due to the three dimensional nature of the experiments and the non-linear magnetic susceptibility of the ferrofluid. Nevertheless, according to the results, we believe our numerical model is capable of quantitatively predicting the behavior of three dimensional droplets with substantially reduced time to investigate a wide range of parameter space.

B. Droplet in simple shear flow with a magnetic field perpendicular to the flow

When a magnetic field is applied to a ferrofluid droplet suspended in a simple shear flow, the droplet deforms due to the combined effects of the magnetic and flow fields. In this section, we first investigate the case where the magnetic field is perpendicular to the flow direction (i.e., $\alpha = 90°$) and has a field strength of $H = 2.5 \times 10^4$ A/m. Two different shear rates, $\dot{\gamma} = 50\ \mathrm{s}^{-1}$ and $600\ \mathrm{s}^{-1}$, are used in order to assess the effect of the magnetic field for different capillary numbers.

Figure 5 represents the effect of the magnetic field in a simple shear flow on the deformation of the ferrofluid droplet. First, the droplet takes a longer time to reach equilibrium shapes, which is consistent with previous findings.[41] Second, the presence of the magnetic field tends to increase the droplet deformation, as seen in Fig. 5(b). When Ca = 0.0194, the deformation parameter of the ferrofluid droplet D under the magnetic field was found to be equal to 0.0988, which was approximately 5 times that of the deformation without a magnetic field. On the other hand, when Ca = 0.2333, the deformation D was found to be 0.2690, which was approximately 1.2 times greater than the shear flow without the magnetic field. The reason behind this comparatively small increase in deformation at a large capillary number is the decrease in the Mason number, $\mathrm{Mn} = \mathrm{Bo}_m/\mathrm{Ca}$. The magnetic field is more dominant than the shear flow for small capillary numbers.

We also compared the deformation of the droplet with an asymptotic theory derived by Jesus *et al.*[41] According to them, the deformation parameter of a ferrofluid droplet in a shear flow in the presence of a perpendicular magnetic field is given by

$$D = \frac{\sqrt{[\alpha(\lambda)\mathrm{Ca}]^2 + [\beta(\chi_d)\mathrm{Bo}_m]^2}}{2 + \frac{1}{3}\beta(\chi_d)\mathrm{Bo}_m}, \tag{23}$$

where $\alpha(\lambda)$ and $\beta(\chi_d)$ are the functions of the viscosity ratio (λ) and the magnetic susceptibility (χ_d) of the droplet which can be written as follows:

$$\alpha(\lambda) = \frac{19\lambda + 16}{8(\lambda + 1)}, \tag{24}$$

$$\beta(\chi_d) = \frac{3\chi_d(2\chi_d + 1)}{4(\chi_d + 3)^2}. \tag{25}$$

Figure 6 shows a comparison of the droplet deformation between our numerical simulations and the asymptotic theory. It can be seen from Fig. 6(a) that for a small capillary number (Ca = 0.0194), the simulation results and the theory given by Jesus *et al.*[41] agree very well with each other. For the large capillary number (Ca = 0.2333), the two results show a large discrepancy with each other. This is because the theory derived by Jesus *et al.* is valid for small capillary numbers and low magnetic field strengths.[41]

Figure 7 presents the velocity field and magnetic field at a steady state for Ca = 0.0194, Re = 0.0015 and Ca = 0.2333, Re = 0.018 at $\mathrm{Bo}_m = 1.4549$. There is circulation inside the droplet due to the surrounding flow on the outside of the ferrofluid droplet. The arrow in the velocity field plot denotes the direction of the velocity in the flow domain. The droplet experiences maximum shear stress and vorticity on the poles of the droplet. From the magnetic field plots, it is clear that the magnetic field is uniform both inside and outside of the droplet. The magnetic field lines are parallel to each other outside the droplet, while these lines are slightly deflected along the interface of the droplet. The droplet experiences maximum magnetic field strength at the interface along the poles of the droplet, while the magnetic field strength is least in magnitude along the equator of the droplet. These characteristics occur because the magnetic field is applied perpendicular to the flow domain ($\alpha = 90°$), which further causes the largest ferrofluid droplet deformation along the poles of the droplet. Also, when

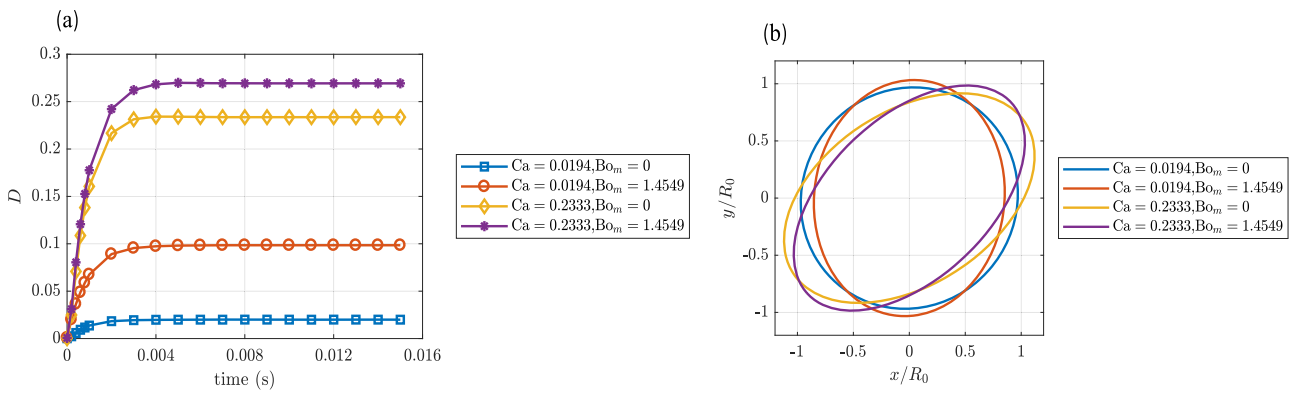

FIG. 5. Effect of a perpendicular magnetic field on the deformation of a ferrofluid droplet in a simple shear flow. (a) Deformation parameter D as a function of time and (b) outline of the droplet shape at a steady state.

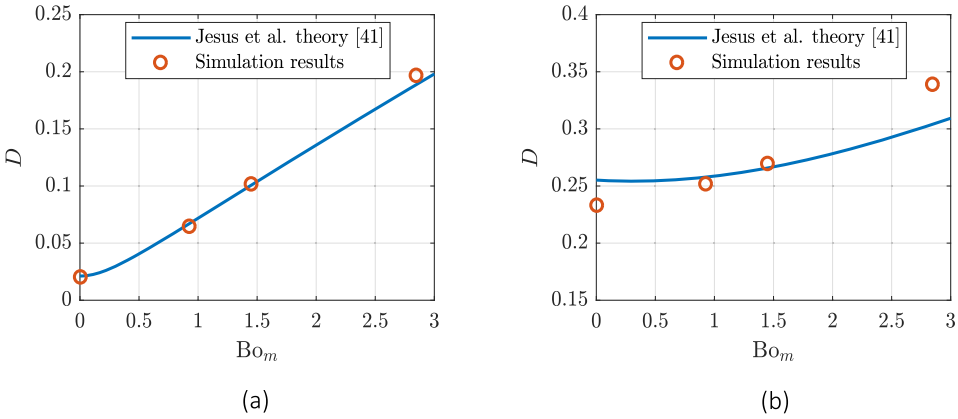

FIG. 6. Comparison of simulation results against the theory given by Jesus *et al.*[41] of droplet deformation when $\alpha = 90°$. (a) D vs Bo$_m$ at Ca = 0.0194 and (b) D vs Bo$_m$ at Ca = 0.2333.

the capillary number is low (Ca = 0.0194), the magnetic field takes control of the deformation of the droplet. As a result, the droplet tends to orient itself along the direction of the applied magnetic field.

C. Effect of the magnetic field at arbitrary directions at a low shear rate (Ca ≈ 0.02)

We now apply the magnetic field at different directions relative to the flow direction (varying $\alpha = 0°$ to $\alpha = 180°$) and examine its effects on the deformation and orientation angle of the droplet under a small shear condition (Ca = 0.0194). In the simulation, α is varied from 0° to 180° at an increment of 15°. However, for better illustration, we chose to present representative α to discuss the effect of the magnetic field on the droplet deformation and orientation. In Fig. 8(a), we can see that at a lower magnetic field strength (Bo$_m$ = 0.0093), the deformation of the droplet seems the same no matter which direction we apply the magnetic field to the flow domain since in this case, the shear flow is dominant and it alone determines

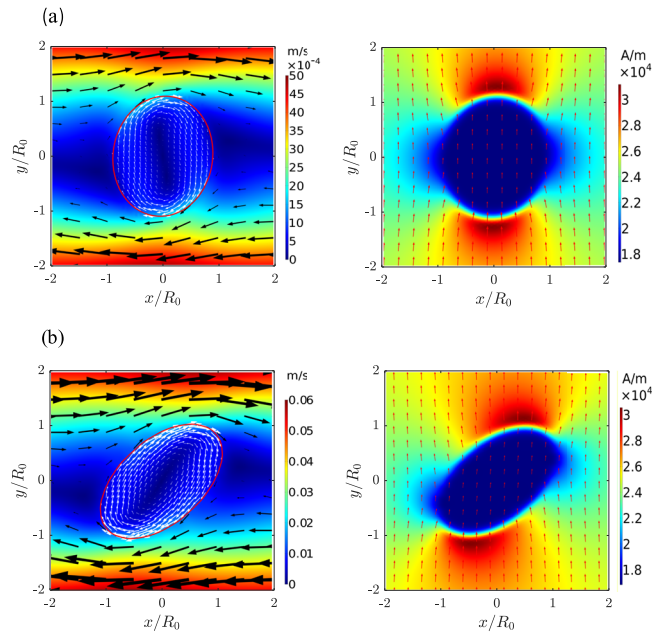

FIG. 7. Velocity field and magnetic field at a steady state. (a) Ca = 0.0194, Re = 0.0015, Bo$_m$ = 1.4549, and $\alpha = 90°$ and (b) Ca = 0.2333, Re = 0.018, Bo$_m$ = 1.4549, and $\alpha = 90°$.

the deformation of the droplet. As we start increasing the magnetic field strength, the deformation profile of the droplet starts to change. In each case, the deformation goes on increasing and attains the maximum value when $\alpha = 45°$. This happens since the shear flow also tends to deform the droplet along 45°, and in this case, the magnetic field additionally aids the droplet to deform more along the same direction. The droplet deformation then starts decreasing as α goes on increasing and attains the minimum value at $\alpha = 135°$. This happens because we are trying to apply the magnetic field along the direction opposite to the favorable direction of the shear flow, and at $\alpha = 135°$, the magnetic field direction becomes exactly opposite to the shear flow. This is why the deformation gains minimum value at this point. This is true for every case as we go on increasing the magnetic field strength up to Bo$_m$ = 5.8194. The deformation D increases with increasing magnetic field strength no matter the direction along which we apply the magnetic field which is due to the dominant nature of the magnetic field at a low shear rate (the Mason number, Mn, increases as we increase the magnetic field strength).

Figure 8(b) gives a clear illustration on the orientation of the droplet for different conditions. For a fixed α, the orientation of the droplet decreases as we go on increasing the magnetic field strength up to $\alpha = 45°$. This is because when the shear rate is low, as the magnetic field strength goes on increasing, the droplet tends to align itself along the direction of the magnetic field direction. Therefore, the resultant between the direction of the shear flow and the direction of the magnetic field decreases [i.e., the orientation angle (θ) of the droplet decreases]. At $\alpha = 45°$, the orientation angle θ reaches a saturation point, and at this point, the orientation of the droplet is independent of the strength of the magnetic field. After that, as α increases up to 135°, the orientation angle θ of the droplet starts increasing with the increase in the magnetic field strength. The reason is due to the dominant nature of the magnetic field as a result of which the resultant between the shear flow direction and the magnetic field direction increases [i.e., the orientation angle (θ) of the droplet increases]. At $\alpha = 135°$, the orientation angle reaches a saturation point again. Figure 9 represents the velocity field and the magnetic field strength at a steady state for Ca = 0.0194, Re = 0.0015, and Bo$_m$ = 1.4549, respectively, for different values of α. These profiles give us a clear visualization about the deformation and orientation of the droplet. At $\alpha = 45°$, the magnetic field lines

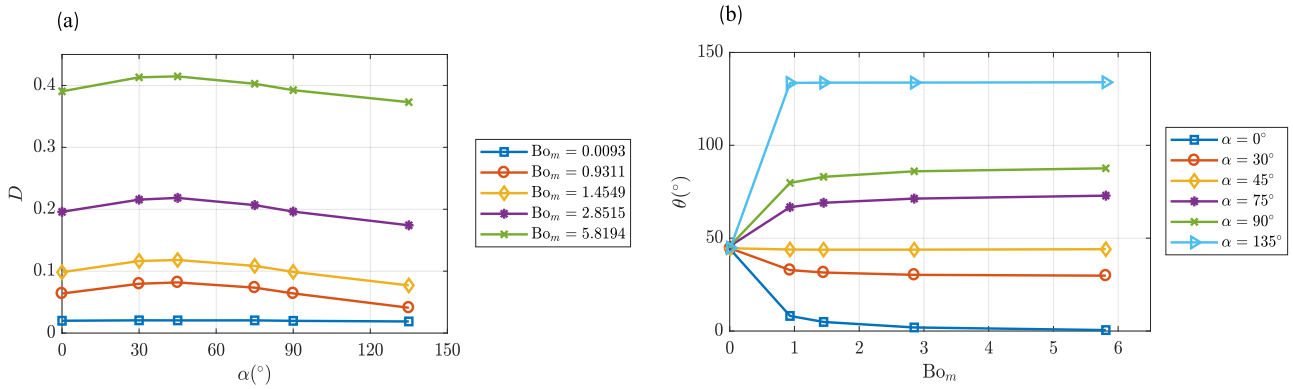

FIG. 8. Effect of the magnetic field at arbitrary directions on the deformation and orientation of the droplet for Ca = 0.0194, Re = 0.0015. (a) Deformation parameter D versus α and (b) orientation angle θ versus Bo_m.

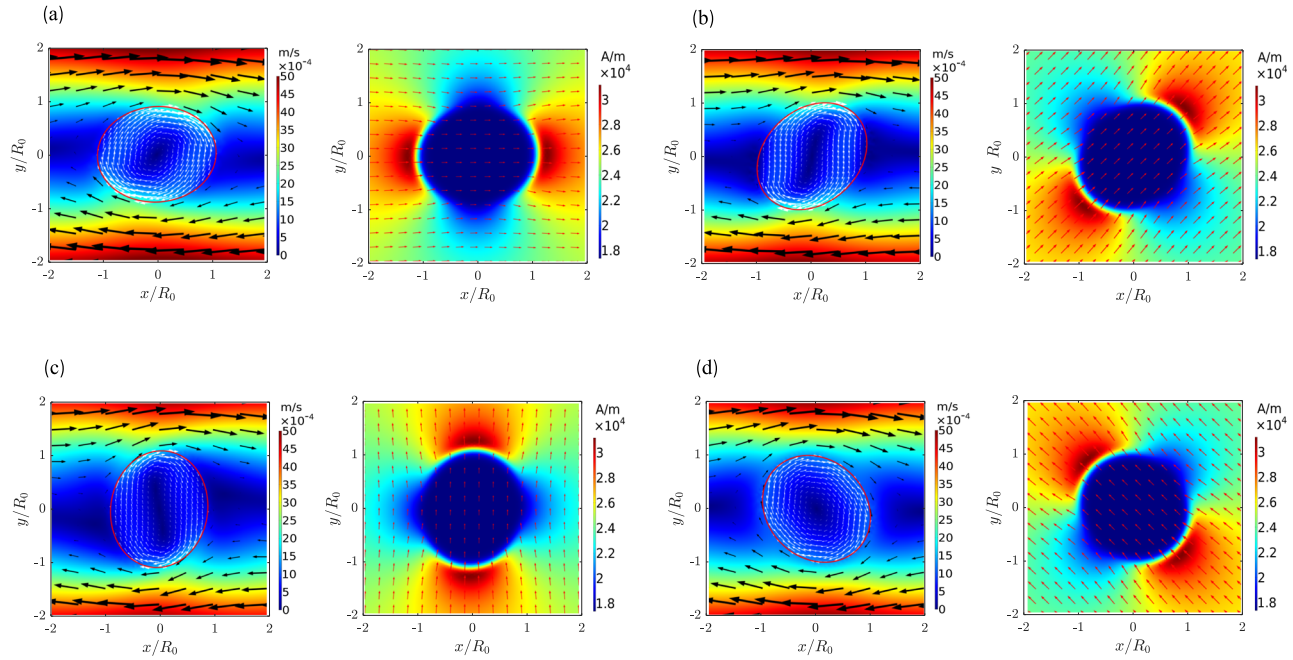

FIG. 9. Velocity field and magnetic field at a steady state for Ca = 0.0194, Re = 0.0015, and Bo_m = 1.4549. (a) α = 0°; (b) α = 45°; (c) α = 90°; and (d) α = 135°.

are trying to deform the droplet in the same direction as the shear flow direction (i.e., deformation D becomes maximum), while at α = 135°, the magnetic field lines are in the opposite direction of the shear flow direction, as a result of which the deformation of the droplet D attains a minimum value at this point.

D. Effect of the magnetic field at arbitrary directions at a high shear rate (Ca ≈ 0.25)

Figure 10 represents the effect of the magnetic field at arbitrary directions on the deformation and orientation of the droplet when Ca = 0.2333 and Re = 0.018. In this case, α was varied from 0° to 180°. From Fig. 10(a), it can be seen that at a lower magnetic field strength (Bo_m = 0.0093), the deformation remains more or less the same regardless of the direction of the magnetic field because in this case, the shear flow alone takes control of the deformation and orientation of the droplet. The magnetic field has more significant influence on the ferrofluid droplet as the magnetic field strength increases (i.e., increasing Bo_m). At a fixed Bo_m, the deformation of the droplet increases and reaches a maximum value at α = 45° and then decreases to a minimum value at α = 135°. Such a variation could be explained by considering the "superposition" effects between the deformation due to the shear flow and deformation due to the magnetic field. Without a magnetic field, the shear flow always tends to elongate the droplet along (or nearly) 45°. On the other hand, the magnetic field always elongates the droplet along the field direction α. As a consequence, when α = 45°, the two effects coincide, yielding the largest deformation, while at α = 135°, the two effects will counteract with each other, thus producing the smallest deformation.

Figure 10(b) shows the orientation of the droplet for different cases. From Fig. 10(b), we can see that for $\alpha \in (5°, 45°)$ and at a fixed α, the orientation angle (θ) of the droplet

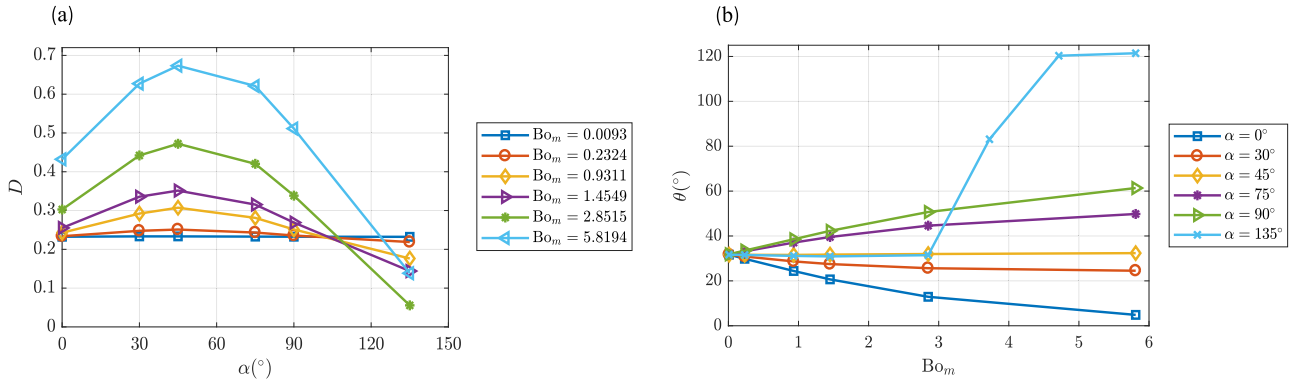

FIG. 10. Effect of the magnetic field at arbitrary directions on the deformation and orientation of the droplet for Ca = 0.2333, Re = 0.018. (a) Deformation D vs α and (b) orientation θ vs Bo_m.

decreases with an increasing magnetic bond number, Bo_m. This is because with increasing magnetic field strength, the magnetic field forces the droplet to align toward the direction of the magnetic field and therefore the resultant orientation of the droplet is decreasing due to the effect of both the magnetic field and the shear flow. Comparing these results to our low shear rate results, we can see that the orientation angle values in this case vary in a smaller range (from 10° to 50°) for the same range of magnetic bond numbers than the values at small capillary numbers (see Fig. 8). This is because the shear flow has a significant effect on the orientation of the droplet at a high capillary number. At $\alpha = 45°$, the orientation angle is predominantly determined by the shear flow alone and has a value close to $\theta \approx 30°$ [similar to Fig. 3(c)]. As α approaches 90°, the orientation angle (θ) of the droplet increases with increasing Bo_m, which can be explained by the "superposition" effect of both the magnetic field and the shear flow. At $\alpha = 135°$, the orientation angle of the droplet seems to reach a constant value and attains similar values as $\alpha = 45°$ up to magnetic bond number $\mathrm{Bo}_m = 2.8515$. The slight discrepancy in the values could be due to the effect of the magnetic field strength at an opposite direction to the shear flow. However, when we apply a very large magnetic field ($\mathrm{Bo}_m > 2.8515$) at $\alpha = 135°$, a sudden jump in the orientation angle values was observed. For example, at a magnetic bond number $\mathrm{Bo}_m = 3.7244$, the orientation angle of the droplet θ was found to be approximately 83°. The reason for this sudden change in the orientation angle can be attributed to the fact that the shear flow is trying to orient the droplet along 30° [Fig. 3(c)], while the magnetic field effect on the orientation of the droplet acts along 135°. As the magnetic field strength gets stronger, its effect on the orientation of the droplet becomes more dominant than the shear flow effect, resulting in a sudden jump in the orientation angle values. As a result, the orientation angle value of the droplet was found to be closer to 135° than 30° at magnetic bond number $\mathrm{Bo}_m = 5.8194$. Additionally, since the deformation of the droplet is also related to the orientation angle, the deformation of the droplet at magnetic bond number $\mathrm{Bo}_m = 5.8194$ shows different behaviors than the deformation values at other magnetic bond numbers at $\alpha = 135°$ although it reaches a minimum value at that point. Figure 11 shows the corresponding velocity field and magnetic field for different values of α. It is seen that at $\alpha = 45°$, the magnetic field lines tend to deform the droplet in the same direction as the shear flow. On the other hand, at $\alpha = 135°$, the magnetic field lines are acting in an opposite direction to the shear flow, and as a result, the deformation of the droplet becomes minimum at this point. Also, due to the counter-effect of the magnetic field with the flow field, the shape of the droplet becomes more rounded than elliptical in this case.

E. Lateral migration of ferrofluid droplets in shear flows

In this section, we demonstrate the feasibility of controlling the lateral migration of ferrofluid droplets in the combined flow and magnetic fields. Recent studies have demonstrated a novel way to manipulate nonspherical *rigid* particles by combining a uniform magnetic field and shear flows at the microscale.[53–55] Although uniform fields exert no forces, a nonzero magnetic torque alters the particle's rotational dynamics and influences the lateral migration of the particle via particle-wall hydrodynamic interactions. Unlike rigid particles, deformable droplets do not rotate but assume a deformed shape at an inclination angle, as seen in Secs. III C and III D. It is expected that a uniform magnetic field can effectively control the orientation angle in a similar way as for rigid particles and can influence the lateral migration.

To investigate the lateral migration behaviors, we consider the motion of the neutrally buoyant ferrofluid droplet between two plane walls with the bottom wall being fixed and the top wall moving at constant velocity, yielding a constant shear rate of 50 s^{-1}. To reduce the entrance effect, the droplet is placed far away from the left boundary, with a vertical position $y = 100$ μm below the center of the flow domain. Periodic flow condition is applied to both the left and right boundaries. Keeping all other parameters and properties of the droplet and continuous phases fixed, the effect of different magnetic field strengths at two different directions, 45° and 135°, on the lateral migration of the droplet is studied.

Figure 12 shows the effect of different magnetic field strengths on the lateral migration of the droplet at a low capillary number (i.e., Ca = 0.0194). The corresponding droplet

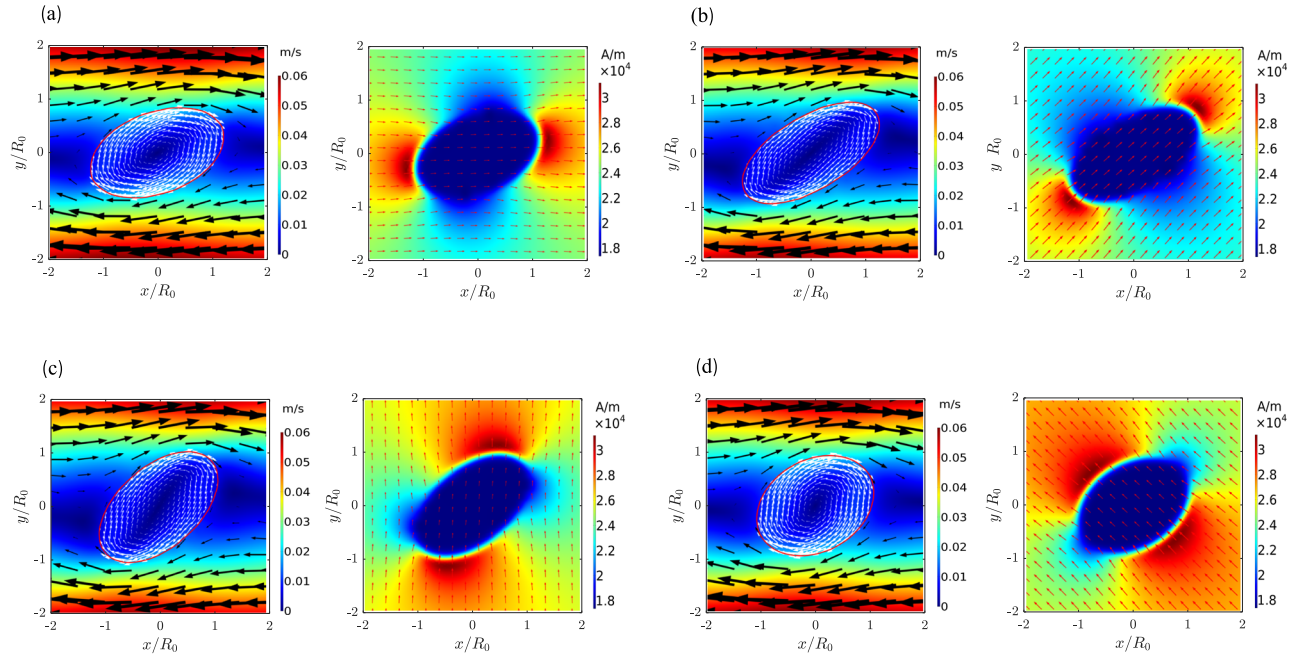

FIG. 11. Velocity field and magnetic field strength at a steady state for Ca = 0.2333, Re = 0.018, and Bo_m = 1.4549. (a) $\alpha = 0°$; (b) $\alpha = 45°$; (c) $\alpha = 90°$; and (d) $\alpha = 135°$.

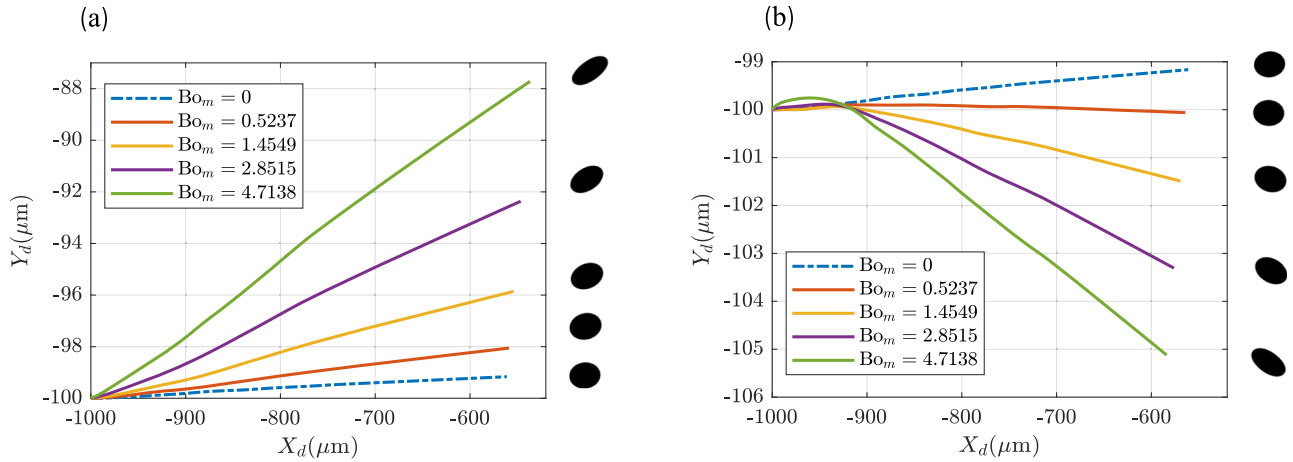

FIG. 12. Effect of different magnetic field strengths on the lateral migration of the droplet at Ca = 0.0194. (a) Y_d vs X_d at $\alpha = 45°$ and (b) Y_d vs X_d at $\alpha = 135°$.

shape at different magnetic field strengths is plotted next to each case. Without a magnetic field, the droplet migrates away from the bottom wall while also moving along the shear flow direction, which is consistent with existing theories in the literature. With a magnetic field applied, Fig. 12(a) shows that when $\alpha = 45°$, the ferrofluid droplet laterally migrates faster toward the center with increasing magnetic field strengths, while at $\alpha = 135°$ [Fig. 12(b)], the droplet migrates faster toward the bottom wall. Also, at $\alpha = 45°$, the magnitude of the migration velocity of the droplet is found to be greater than at $\alpha = 135°$ for the same magnetic bond number. For example, when the magnetic bond number Bo_m was equal to 2.8515, the migration velocity of the droplet is found to be 126.92 μm/s and 74.97 μm/s at $\alpha = 45°$ and 135°, respectively. These different lateral migration behaviors of the droplet are related to the orientation and deformation of the droplet and the hydrodynamic interactions between the droplet and wall[56] and will be investigated in future work.

Furthermore, we experimentally demonstrate that the uniform magnetic field can control the lateral migration of ferrofluid droplets in a microchannel, which is in qualitative agreement with our numerical results. In our experiment, a microfluidic chip was fabricated with polydimethylsiloxane (PDMS) using the soft-lithography method.[57,58] The main microchannel had a width of 300 μm, a depth of 70 μm, and a total length of about 14 000 μm. A uniform magnetic field was generated by a Halbach array,[59] which consisted of 20 cuboid permanent 0.25″ × 0.25″ × 1″ magnets (K&J Magnetics, Inc.). The magnitude of the magnetic field within the central region was H ≈ 60 000 A/m which is measured by using a gaussmeter. Ferrofluid (EMG 304, Ferrotec Corp.)

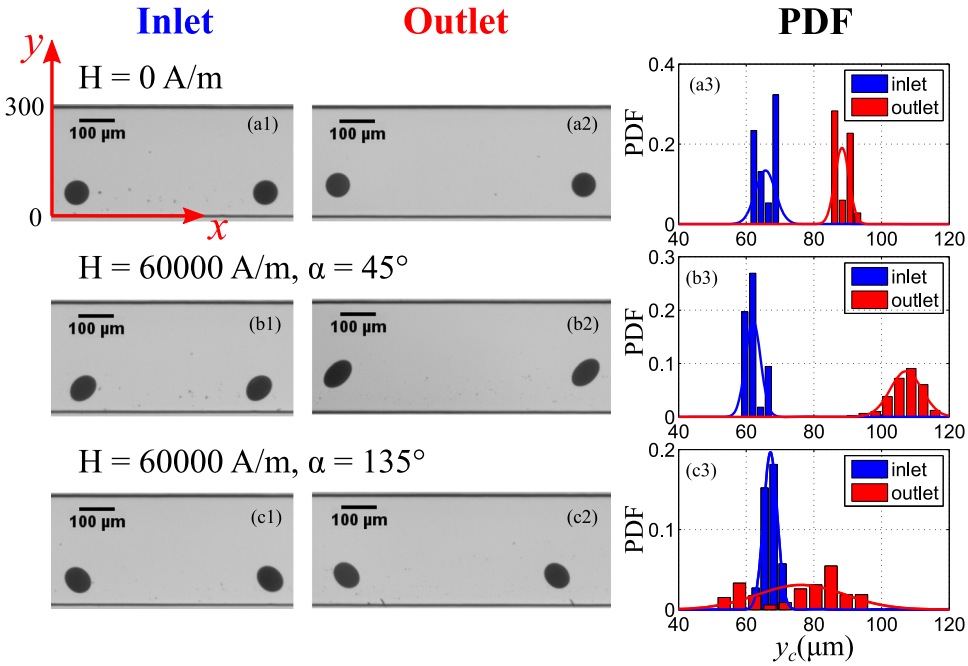

FIG. 13. Images at the inlet and outlet and the corresponding probability density function (PDF) of the ferrofluid droplet centroid in the y direction. [(a1)–(a3)] without a magnetic field (H = 0 A/m); [(b1)–(b3)] a magnetic field (H ≈ 60 000 A/m) is applied at $\alpha = 45°$; and [(c1)–(c3)] a magnetic field (H ≈ 60 000 A/m) is applied at $\alpha = 135°$. The total flow rate was 6 μl/min for all experiments.

droplets were generated by a T-junction configuration and were dispersed and transported by a continuous phase made of olive oil. The density, viscosity, and magnetic susceptibility of the ferrofluid are 1.24×10^3 kg/m^3, 5×10^{-3} Pa s, and 5.03, respectively. The density, viscosity, and magnetic susceptibility of the olive oil are 0.92×10^3 kg/m^3, 78×10^{-3} Pa s, and 0, respectively. The total flow rate was 6 μl/min for all experiments, so the corresponding Reynolds number is 0.23. Surfactant SPAN 80 (Sigma-Aldrich, USA) is added to the olive oil at 0.25% w/w to decrease the interfacial tension between the olive oil and ferrofluid. The interfacial tension between the two fluids is measured as 10.26 ± 0.81 mN/m.

Figure 13 shows the images of droplets at the inlet and outlet and the corresponding probability distributions of the droplet centroid in the y direction. The average radius of the un-deformed droplet is 34.98 μm, so the Reynolds number, capillary number, and magnetic bond number of the droplet are calculated to be 6.18×10^{-4}, 0.0084, and 7.72, respectively. As can be seen in Figs. 13(a1)–13(a3), there is a slight deformation of the droplet and a net lateral migration in the y direction. The nonlinear velocity profile is the reason for the deformation. The inertia effect is the major reason for the net lateral migration. When the magnetic field is applied at $\alpha = 45°$, as shown in Figs. 13(b1)–13(b3), the droplet tends to deform in the direction of magnetic field, and the degree of deformation is larger than that without a magnetic field. The net lateral migration in the y direction becomes larger compared to the result without a magnetic field. When the magnetic field is applied at $\alpha = 135°$, as shown in Figs. 13(c1)–13(c3), we observe elongation along $\alpha = 135°$, and the net lateral migration in the y direction becomes smaller compared to the result without a magnetic field. These findings are qualitatively consistent with the numerical predictions although the parameters used in the experiments are different from those in the numerical simulations.

IV. CONCLUSION

The influence of the magnetic field on the droplet deformation and orientation angle based on the arbitrary field direction, magnetic bond number, and capillary number in a simple shear flow is systematically studied in this paper. At a small capillary number (Ca ≈ 0.02), the magnetic field plays a significant role and dictates the deformation and orientation of the droplet. Also, as we increase the magnetic field strength at a fixed magnetic field direction α, the deformation of the droplet increases, whereas at a fixed magnetic bond number Bo$_m$, the orientation angle of the droplet increases with increasing α. At a large capillary number (Ca ≈ 0.25), the deformation and orientation of the droplet is determined by both the shear flow and the magnetic field. In particular, the effect of the magnetic field is substantially observed at a higher magnetic bond number, Bo$_m$. At a fixed α with increasing magnetic field strength, the deformation of the droplet increases up to $\alpha = 90°$ and decreases at $\alpha = 135°$, whereas the orientation angle of the droplet at a fixed Bo$_m$ increases with increasing α up to 90°. At $\alpha = 135°$, it attains similar values as $\alpha = 45°$ except at large magnetic bond numbers (i.e., Bo$_m$ > 2.8515). The orientation angle values are much lower in this case compared to a low shear rate due to the dominant nature of the shear flow. In both cases, the deformation of the droplet attains a maximum value at $\alpha = 45°$ and becomes minimum at $\alpha = 135°$. Additionally, the flow field both inside and outside of the droplet is modified according to the deformation and orientation of the droplet. We also investigated the lateral migration of the ferrofluid droplet in wall-bounded shear flows in the presence of a magnetic field both numerically and experimentally and found that at $\alpha = 45°$, the droplet migrates toward the center of the domain, while at $\alpha = 135°$, the droplet migrates toward the wall. The magnitude of the migration velocity was also found to increase with increasing magnetic field strength. The different lateral migration behaviors of the droplet provide a

simple but an effective way to separate ferrofluid droplets from nonmagnetic droplets at microscale.

ACKNOWLEDGMENTS

The authors gratefully acknowledge the financial support from the Department of Mechanical and Aerospace Engineering (MAE) and the Center for Biomedical Research (CBR) at Missouri University of Science and Technology.

[1]A. Lamura, G. Gonnella, and J. Yeomans, "A lattice Boltzmann model of ternary fluid mixtures," Europhys. Lett. **45**, 314 (1999).
[2]K. Mosbach and L. Andersson, "Magnetic ferrofluids for preparation of magnetic polymers and their application in affinity chromatography," Nature **270**, 259 (1977).
[3]R. Van der Sman and S. Van der Graaf, "Diffuse interface model of surfactant adsorption onto flat and droplet interfaces," Rheol. Acta **46**, 3–11 (2006).
[4]R. Van der Sman and S. Van der Graaf, "Emulsion droplet deformation and breakup with lattice Boltzmann model," Comput. Phys. Commun. **178**, 492–504 (2008).
[5]P. Yue, J. J. Feng, C. Liu, and J. Shen, "A diffuse-interface method for simulating two-phase flows of complex fluids," J. Fluid Mech. **515**, 293–317 (2004).
[6]J. M. Rallison, "The deformation of small viscous drops and bubbles in shear flows," Annu. Rev. Fluid Mech. **16**, 45–66 (1984).
[7]H. A. Stone, "Dynamics of drop deformation and breakup in viscous fluids," Annu. Rev. Fluid Mech. **26**, 65–102 (1994).
[8]G. I. Taylor, "The viscosity of a fluid containing small drops of another fluid," Proc. R. Soc. A **138**, 41–48 (1932).
[9]G. Taylor, "The formation of emulsions in definable fields of flow," Proc. R. Soc. A **146**, 501–523 (1934).
[10]F. D. Rumscheidt and S. G. Mason, "Particle motions in sheared suspensions XII. Deformation and burst of fluid drops in shear and hyperbolic flow," J. Colloid Sci. **16**, 238–261 (1961).
[11]R. A. De Bruijn, "Tipstreaming of drops in simple shear flows," Chem. Eng. Sci. **48**, 277–284 (1993).
[12]V. Sibillo, G. Pasquariello, M. Simeone, V. Cristini, and S. Guido, "Drop deformation in microconfined shear flow," Phys. Rev. Lett. **97**, 054502 (2006).
[13]D. Barthes-Biesel and A. Acrivos, "Deformation and burst of a liquid droplet freely suspended in a linear shear field," J. Fluid Mech. **61**, 1–22 (1973).
[14]H. Xi and C. Duncan, "Lattice Boltzmann simulations of three-dimensional single droplet deformation and breakup under simple shear flow," Phys. Rev. E **59**, 3022 (1999).
[15]J. Li, Y. Y. Renardy, and M. Renardy, "Numerical simulation of breakup of a viscous drop in simple shear flow through a volume-of-fluid method," Phys. Fluids **12**, 269–282 (2000).
[16]A. J. Griggs, A. Z. Zinchenko, and R. H. Davis, "Low-Reynolds-number motion of a deformable drop between two parallel plane walls," Int. J. Multiphase Flow **33**, 182–206 (2007).
[17]K. Feigl, D. Megias-Alguacil, P. Fischer, and E. J. Windhab, "Simulation and experiments of droplet deformation and orientation in simple shear flow with surfactants," Chem. Eng. Sci. **62**, 3242–3258 (2007).
[18]R. A. Debruijn, "Deformation and breakup of drops in simple shear flows," Ph.D. thesis, Technische University, Eindhoven, The Netherlands, 1991.
[19]H. A. Stone, J. R. Lister, and M. P. Brenner, "Drops with conical ends in electric and magnetic fields," Proc. R. Soc. A **455**, 329–347 (1999).
[20]S. Mählmann and D. T. Papageorgiou, "Numerical study of electric field effects on the deformation of two-dimensional liquid drops in simple shear flow at arbitrary Reynolds number," J. Fluid Mech. **626**, 367–393 (2009).
[21]P. M. Vlahovska, "On the rheology of a dilute emulsion in a uniform electric field," J. Fluid Mech. **670**, 481–503 (2011).
[22]S. Mandal, A. Bandopadhyay, and S. Chakraborty, "The effect of uniform electric field on the cross-stream migration of a drop in plane Poiseuille flow," J. Fluid Mech. **809**, 726–774 (2016).
[23]S. Mandal and S. Chakraborty, "Effect of uniform electric field on the drop deformation in simple shear flow and emulsion shear rheology," Phys. Fluids **29**, 072109 (2017).
[24]J.-C. Bacri, D. Salin, and R. Massart, "Study of the deformation of ferrofluid droplets in a magnetic field," J. Phys., Lett. **43**, 179–184 (1982).
[25]S. Afkhami, A. Tyler, Y. Renardy, M. Renardy, T. S. Pierre, R. Woodward, and J. Riffle, "Deformation of a hydrophobic ferrofluid droplet suspended in a viscous medium under uniform magnetic fields," J. Fluid Mech. **663**, 358–384 (2010).
[26]Y. I. Dikansky, A. N. Tyatyushkin, and A. R. Zakinyan, "Anisotropy of magnetic emulsions induced by magnetic and electric fields," Phys. Rev. E **8**, 031402 (2011).
[27]A. Zakinyan and Y. Dikansky, "Drops deformation and magnetic permeability of a ferrofluid emulsion," Colloids Surf., A **380**, 314–318 (2011).
[28]A. Zakinyan, Y. Dikansky, and M. Bedzhanyan, "Electrical properties of chain microstructure magnetic emulsions in magnetic field," J. Dispersion Sci. Technol. **35**, 111–119 (2014).
[29]R. E. Rosensweig, *Ferrohydrodynamics* (Cambridge University Press, 1985).
[30]O. T. Mefford, R. C. Woodward, J. D. Goff, T. Vadala, T. G. S. Pierre, J. P. Dailey, and J. S. Riffle, "Field-induced motion of ferrofluids through immiscible viscous media: Testbed for restorative treatment of retinal detachment," J. Magn. Magn. Mater. **311**, 347–353 (2007).
[31]V. Varma, A. Ray, Z. Wang, Z. Wang, and R. Ramanujan, "Droplet merging on a lab-on-a-chip platform by uniform magnetic fields," Sci. Rep. **6**, 37671 (2016).
[32]J. Liu, Y. F. Yap, and N.-T. Nguyen, "Numerical study of the formation process of ferrofluid droplets," Phys. Fluids **23**, 072008 (2011).
[33]Y. Wu, T. Fu, Y. Ma, and H. Z. Li, "Ferrofluid droplet formation and breakup dynamics in a microfluidic flow-focusing device," Soft Matter **9**, 9792–9798 (2013).
[34]S.-H. Tan, N.-T. Nguyen, L. Yobas, and T. G. Kang, "Formation and manipulation of ferrofluid droplets at a microfluidic t-junction," J. Micromech. Microeng. **20**, 045004 (2010).
[35]Q. Zhang, H. Li, C. Zhu, T. Fu, Y. Ma, and H. Z. Li, "Micro-magnetofluidics of ferrofluid droplet formation in a T-junction," Colloids Surf., A **537**, 572–579 (2018).
[36]A. Ghaffari, S. H. Hashemabadi, and M. Bazmi, "CFD simulation of equilibrium shape and coalescence of ferrofluid droplets subjected to uniform magnetic field," Colloids Surf., A **481**, 186–198 (2015).
[37]S. Afkhami, Y. Renardy, M. Renardy, J. Riffle, and T. St Pierre, "Field-induced motion of ferrofluid droplets through immiscible viscous media," J. Fluid Mech. **610**, 363–380 (2008).
[38]D. Shi, Q. Bi, and R. Zhou, "Numerical simulation of a falling ferrofluid droplet in a uniform magnetic field by the VOSET method," Numer. Heat Transfer, Part A **66**, 144–164 (2014).
[39]M. S. Korlie, A. Mukherjee, B. G. Nita, J. G. Stevens, A. D. Trubatch, and P. Yecko, "Modeling bubbles and droplets in magnetic fluids," J. Phys.: Condens. Matter **20**, 204143 (2008).
[40]G.-P. Zhu, N.-T. Nguyen, R. V. Ramanujan, and X.-Y. Huang, "Nonlinear deformation of a ferrofluid droplet in a uniform magnetic field," Langmuir **27**, 14834–14841 (2011).
[41]W. C. Jesus, A. M. Roma, and H. D. Ceniceros, "Deformation of a sheared magnetic droplet in a viscous fluid," Commun. Comput. Phys. **24**, 332–355 (2017).
[42]R. Van Der Sman, S. van Der Graaf, and A. Gijsbertsen-Abrahamse, "2-d droplet deformation and breakup with lattice Boltzmann model," WIT Trans. Eng. Sci. **42**, 333–342 (2003).
[43]M. Ansari, A. Hadidi, and M. Nimvari, "Effect of a uniform magnetic field on dielectric two-phase bubbly flows using the level set method," J. Magn. Magn. Mater. **324**, 4094–4101 (2012).
[44]S. Osher and R. P. Fedkiw, "Level set methods: An overview and some recent results," J. Comput. Phys. **169**, 463–502 (2001).
[45]COMSOL, *CFD Module Application Library Manual*, 5th ed. (2017).
[46]E. Olsson and G. Kreiss, "A conservative level set method for two phase flow," J. Comput. Phys. **210**, 225–246 (2005).
[47]J. A. Stratton, *Electromagnetic Theory* (John Wiley & Sons, 2007).
[48]M. Kennedy, C. Pozrikidis, and R. Skalak, "Motion and deformation of liquid drops, and the rheology of dilute emulsions in simple shear flow," Comput. Fluids **23**, 251–278 (1994).
[49]S. Guido and M. Villone, "Three-dimensional shape of a drop under simple shear flow," J. Rheol. **42**, 395–415 (1998).
[50]A. Vananroye, P. Van Puyvelde, and P. Moldenaers, "Effect of confinement on the steady-state behavior of single droplets during shear flow," J. Rheol. **51**, 139–153 (2007).
[51]R. Cerf, "Recherches théoriques et expérimentales sur l'effet Maxwell des solutions de macromolécules déformables," J. Chim. Phys. **48**, 59–84 (1951).
[52]R. Roscoe, "On the rheology of a suspension of viscoelastic spheres in a viscous liquid," J. Fluid Mech. **28**, 273–293 (1967).

[53]R. Zhou, F. Bai, and C. Wang, "Magnetic separation of microparticles by shape," Lab Chip **17**, 401–406 (2017).
[54]R. Zhou, C. A. Sobecki, J. Zhang, Y. Zhang, and C. Wang, "Magnetic control of lateral migration of ellipsoidal microparticles in microscale flows," Phys. Rev. Appl. **8**, 024019 (2017).
[55]D. Matsunaga, F. Meng, A. Zöttl, R. Golestanian, and J. M. Yeomans, "Focusing and sorting of ellipsoidal magnetic particles in microchannels," Phys. Rev. Lett. **119**, 198002 (2017).
[56]W. Hiller and T. Kowalewski, "An experimental study of the lateral migration of a droplet in a creeping flow," Exp. Fluids **5**, 43–48 (1986).
[57]J. C. McDonald, D. C. Duffy, J. R. Anderson, D. T. Chiu, H. Wu, O. J. Schueller, and G. M. Whitesides, "Fabrication of microfluidic systems in poly (dimethylsiloxane)," Electrophoresis **21**, 27–40 (2000).
[58]R. Zhou and C. Wang, "Acoustic bubble enhanced pinched flow fractionation for microparticle separation," J. Micromech. Microeng. **25**, 084005 (2015).
[59]H. Raich and P. Blümler, "Design and construction of a dipolar Halbach array with a homogeneous field from identical bar magnets: NMR Mandhalas," Concepts Magn. Reson., Part B **23**, 16–25 (2004).